Journal of Ceramic Processing Research. Vol. 21, Special. 1, pp. s41~s46 (2020)
(Received 16 December 2019, Received in revised form 16 April 2020, Accepted 4 May 2020)
https://doi.org/10.36410/jcpr.2020.21.S1.s41

J O U R N A L O F
Ceramic Processing Research

Enhancement of surface roughness of zirconia substrate by slurry coating

Woo Chang Kim and Jong Kook Lee*
Department of Materials Science and Engineering, Chosun University, Gwangju 61452, Korea

In order to increase the bone bonding-ability and biocompatibility of zirconia-based implants, the surface roughness must be high. In this study, we tried to improve the surface roughness of the zirconia substrates by surface modification using two types of zirconia slurry and spin coating. We also investigated to the effect of repeated coating times on the surface roughness of coating layer. Coating layers fabricated by slurry and spin coating showed uniform thickness and dense microstructure. As increasing the repeated coating times, the thickness of coating layer gradually increased from 0.7 to 1.7 μm in case of small particles or from 0.9 to 2.0 μm in case of large particles. Slurry containing small particles (~ 40 nm) had low viscosity and good forming-ability of coating films, but the improvement of surface roughness by slurry coating was not high. Roughness enhancement on coated layer in zirconia slurry containing large particles (~100nm) was higher than that of small particles at the same processing condition. In this study, 4 times coating specimen showed maximum surface roughness of Ra 0.36 μm in 3Y-TZP powder containing large particles, or Ra 0.27 μm in that of small particles.

Keywords: Zirconia Slurry, Solid loading, Spin coating.

Introduction

Zirconia ceramics have promising mechanical properties, including corrosion resistance, wear resistance and high stability and it is a representative ceramic material in various industries [1, 2]. Excellent wear resistance and high fracture toughness of the ceramic materials applied to hip implant balls, bearings, grinding ball and various wear resistant structural materials [3-6]. Additionally, zirconia is white with high light transmittance, low sensitivity to plaque formation, and excellent biocompatibility, suggesting the utilization of dental implant applications [7-10]. Zirconia materials are also used as oxygen sensor and solid fuel cell material by utilizing ion conductivity through oxygen vacancies and is suitable for manufacturing various ceramic related components [11].

Recently, zirconia-based bioceramics are widely used as implant materials because of their effective biological properties such as biocompatibility, minimizing ion release, and low affinity to bacterial colonization [12, 13]. Of the zirconia ceramics, 3mol% yttria stabilized tetragonal ziconia polycrystals (3Y-TZP) is frequently used as a main material for dental ceramic implants. It is also widely studied as a substitute material for titanium implant due to its high refractive index, light transmittance and aesthetics.

Enhanced mechanical and biological properties can be improved by optimizing sintering processes and after surface treatment [14]. 3Y-TZP ceramics has biological bioinertness and shows easy failure during implantation due to the limit of direct bonding between implant and human bone [15-17]. In order to further increase the bone bonding strength and biocompatibility of such zirconia- based implants, surface modification of implants is required [18-20]. The sol-gel and powder slurry coating methods can be manufactured the surface coating of zirconia implant through an inexpensive and simple process, enhancing the bone cohesion and biocompatibility by improving surface roughness [21-22]. Slurry coating provides a relatively thick coating layer and could be controlled the thickness by repeated coating times, and is available to obtain the optimal surface properties for the good induction of bone adhesion during the initial period after implantation. Additionally, thick coating layer from slurry coating process has an advantage to use for long periods due to the relatively slower dissolution rate [23].

The preparation of aqueous slurry is most important in the ceramic slurry coating process, and it should be controlled the slurry pH, dispersant content and solid loading in order to produce a stable and high production efficiency. Sometimes, to supplement the slurry dip coating or sol-gel dip coating, spin coating is used to apply the coating uniformity and dense coating layer. In general, the spin coating is thinly spread on the substrate by the high-speed rotational movement on the substrate to form a coating layer [24-26].

In this study, two types of 3Y-TZP powder with different particle size were used to obtain the 3Y-TZP coating with high surface roughness through the spin

*Corresponding author:
Tel : +82 62-230-7202
Fax: +82 62-608-5402
E-mail: jklee@chosun.ac.kr

coating of aqueous slurry. We also have an expectation to form a uniform and dense coating layer by this surface modification, which improves the bone bonding strength and biocompatibility of zirconia ceramics. In this process, we tried to control the surface microstructure and roughness by change of slurry parameters, i.e. particle type of 3Y-TZP and coating times, and investigated the dependence of processing factors to coating surface and microstructural evolution.

Experimental Details

Two sizes of commercial 3Y-TZP powder were used for zirconia slurry preparation. Powder properties about particle morphology, phase composition and particle size distribution were characterized, and compared to the influence on the slurry and coating properties. Slurry preparation condition obtained from preliminary experiments was used, such as pH 12, 1 wt.% dispersant (Darvan C), and 40 wt.% solid loading. Two types of nanoscale 3Y-TZP powder (40 and 100 nm diameter) were used to prepare the zirconia slurry through ball milling for 24 hours as shown in Fig. 1. Considering the slurry fluidity and coating thickness, the content of solid loading of 3Y-TZP powder was fixed to 40 wt.%, determined from the previous results [27].

The 3Y-TZP substrate for slurry coating was fabricated a disc-type porous specimen by uniaxial pressing and pre-sintering at 1,100 °C for 2 h. Using a spin coater, zirconia slurry was coated on the pre-sintered 3Y-TZP porous specimen, and repeated a spin coating after drying. Maximum coating times at solid loading of 40 wt.% was limited to 8 on the same substrate, considering the variation of surface roughness. Final sintering after coating was carried out at 1,500 °C for 2 hours. Coated microstructure and surface morphology including surface roughness were observed by Scanning Electron Microscope (SEM) and Atomic Force Microscope (AFM), and analyzed the surface microstructure and

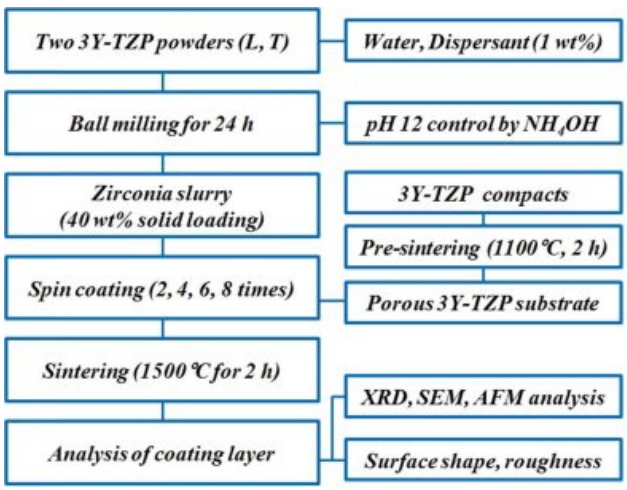

Fig. 1. Schematic flowchart for the experimental procedure.

coating thickness with powder type and coating times. Of the surface parameter from AFM images, the value of Ra (center line average) was selected as a representative parameter of surface roughness. Finally we investigated the influence of processing factors to the surface properties of coated layer.

Results and Discussion

Two types of 3Y-TZP commercial powders with different particle size were used as raw materials for the slurry preparation and their microstructural morphology and agglomeration characterization via particle size distribution analysis were shown in Fig. 2. The first powder containing large scale particles (noted to L powder) showed a severe agglomeration (larger agglomerate size and more secondary agglomerate) and large primary particle size (about 100 nm). The second powder containing small scale particles (note to T powder) is small primary particle size (about 40 nm) and weak agglomeration characteristics. From the analysis of particle size distribution as shown in Fig. 2(a), L powder consists of 83% primary aggregates of 232 nm and 17% secondary aggregates of 2.5 μm. Comparatively, T powder is composed of 94% primary aggregates of 197 nm and 6% secondary aggregates of 1.6 μm.

Fig. 3(a) shows the slurry viscosity at pH 12 as a function of solid loading prepared by mixing and milling of 3Y-TZP powder, distilled water, dispersant and pH control agent. With increasing the solid loading of 3Y-TZP powder, slurry viscosity was gradually increased regardless of powder type. But the slurry including 50wt.% solid loading had high viscosity over 60 cP, which was limited to carry out the spin coating due to the less fluidity of slurry. So, solid loading was fixed to 40 wt.% in this experiment, considering a coating efficiency for a forming-ability of 3Y-TZP thick film. Slurry viscosity for L or T powder containing 40 wt.% solid loading indicated the proper range (about 36 and 27 cP, respectively) for spin coating, and L powder slurry had higher viscosity than that of T powder due to the large particle size and severe agglomeration.

Fig. 3(b) and (c) show the surface microstructure and morphology for zirconia substrate observed by SEM and AFM. Pre-sintered 3Y-TZP substrate at 1,100 °C for 2 h shows porous microstructure with grain size of 175 nm and apparent density of 90%. Porous structure of substrate surface enhances the slurry coating by the capillary force of open pores. From the analysis of AFM images, porous 3Y-TZP substrate had roughened surface (Ra; 0.16 μm). Phase composition of two types of 3Y-TZP powder and pre-sintered substrate presents in Fig. 4(a), indicating a main tetragonal phase and a little minor monoclinic phase in commercial two powders. Phase composition of coated layer after a spin coating and sintering at 1,500 °C for 2 h was slightly different from each other as shown in Fig. 4(b). Coated

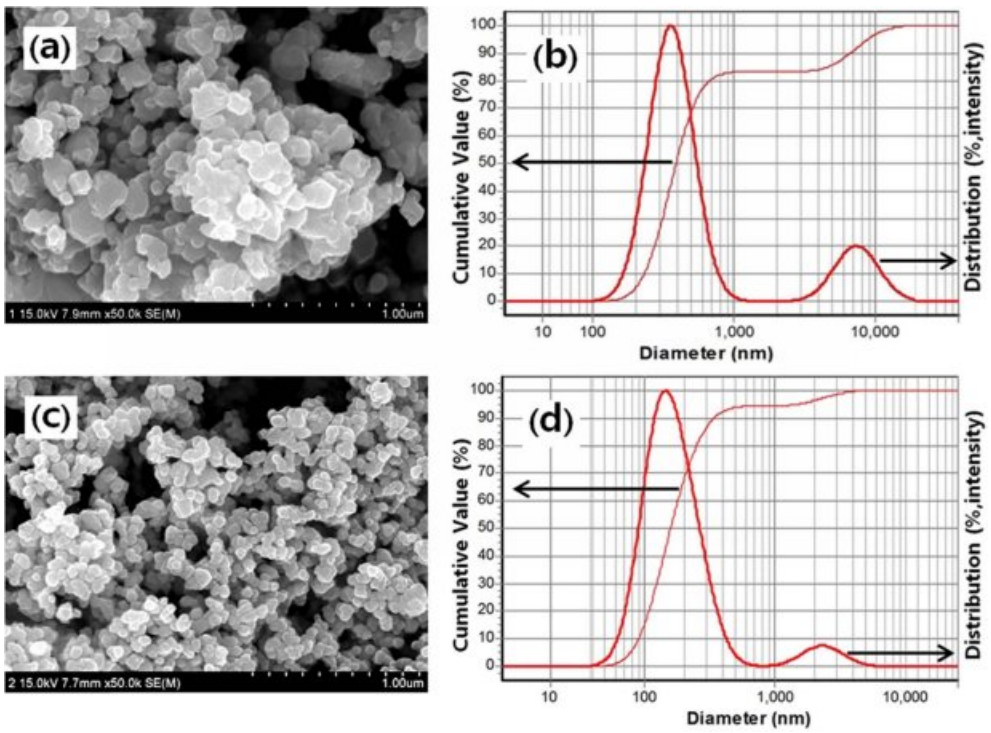

Fig. 2. Particle morphology and particle size distribution analysis of two types of 3Y-TZP commercial powder; (a), (b) L powder, and (c), (d) T powder.

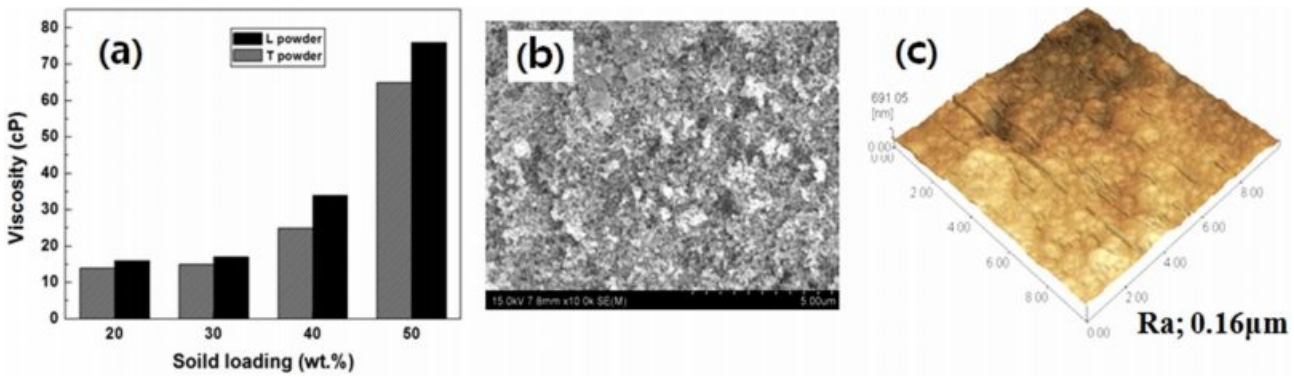

Fig. 3. Characteristics of slurry viscosity and surface morphology of 3Y-TZP substrate; (a) viscosity variation with solid loading of two types of 3Y-TZP powders, (b) porous microstructure of 3Y-TZP substrate and (c) surface morphology by AFM observation.

layer fabricated from L powder indicates a main tetragonal phase and a small quantity of monoclinic phase. The partial existence of monoclinic phase on coating surface is due to the severe agglomeration and the growth of a few large grains during sintering. On the other hand, coated zirconia layer by T powder composed of all tetragonal grains, because of small particles and densification due to the sintering at high temperature.

Fig. 5 shows the surface microstructure and perpendicular fractured surface of coated layer after the post-sintering at 1500°C for 2 hours. 3Y-TZP coated films are homogeneous surface microstructure and uniform thickness, but it depends on the powder type and coating times. In 3Y-TZP coated surface layer fabricated from L powder, the growth of large scale grains was evident and resulted to large average grain size of 650 nm, irrespective of coating times, and the thickness of coating layer was gradually increased from 0.9 to 2.0 μm with increasing coating times. In contrast, coated surface layer fabricated from T powder, small scale grains were mainly observed on surface microstructure, indicating the grain growth inhibition during sintering by soft agglomerates, and resulted to small average grain size of 300 nm. The thickness of coating layer in this powder was also gradually increased from 0.7 to 1.7 μm with increasing coating times.

Surface morphology and roughness analyzed from AFM images were dependent on the powder type and coating times. In comparison with substrate morphology,

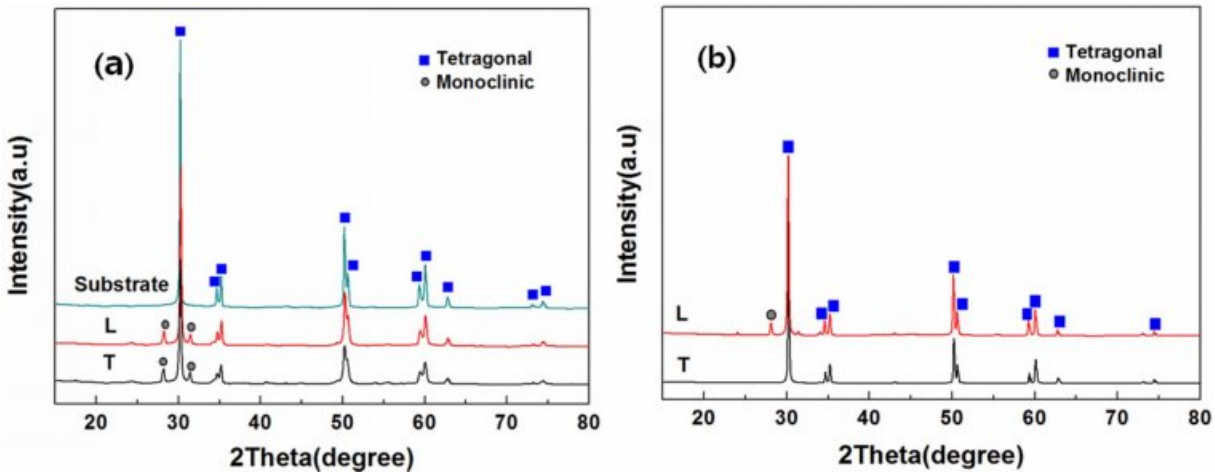

Fig. 4. Phase composition of (a) two types of starting 3Y-TZP powder and pre-sintered substrate, and (b) coated surface after slurry coating.

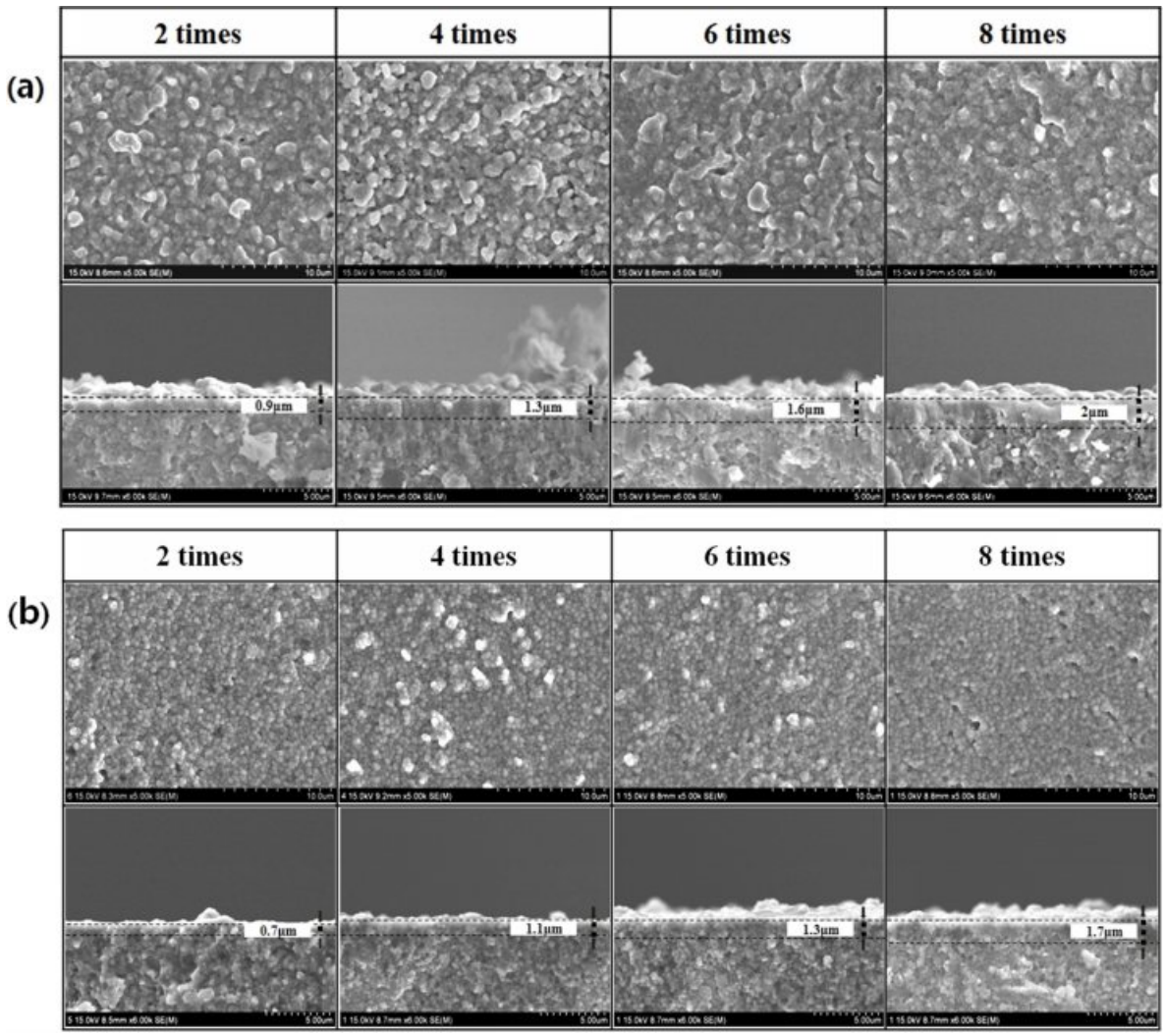

Fig. 5. Variation of surface microstructure and film thickness on coated layer with powder type and coating times; (a) L powder, (b) T powder.

some protruding particles as like a mountain-like shape were observed on coated surface, which number and size were dependent on the type of powder and coating times. Protruding particles formed from L powder in Fig. 6 are larger than that of T powder, meaning that it related with the particle size of starting powder. The

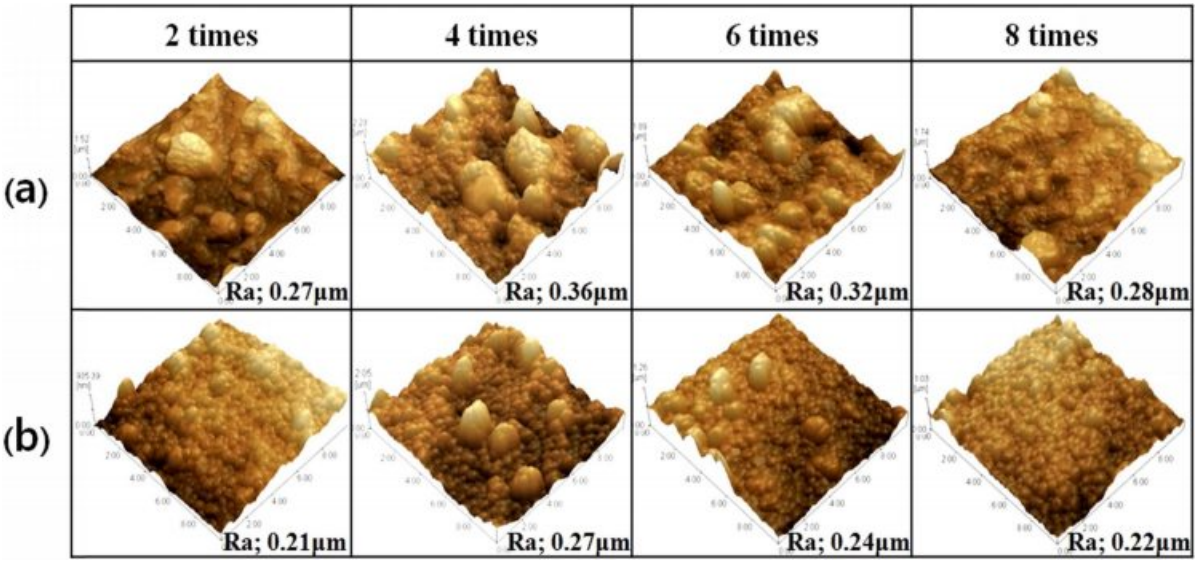

Fig. 6. Variation of surface morphology and roughness on coated layer with powder type and coating times; (a) L powder, (b) T powder.

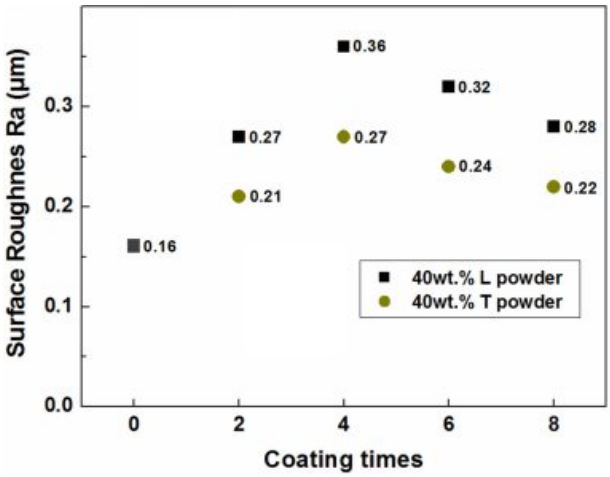

Fig. 7. Dependence of surface roughness (Ra) on the powder type and coating times.

number of protruding particles on coated surface showed the maximum value in 4 times coating specimen, compared with less protruding particles in 2 or 8 times coating specimen. It suggested that the formation and surface appearance of protruding particles were related with the particle deposition during spin coating, that is, particle compaction and arrangement at repeated coating. As shown in AFM images, the number of protruding particles was increased to 4 time coatings in both types of 3Y-TZP powder, but they partially disappeared from the coated surface in 6 or 8 coatings specimen. It means that the formation and surface appearance of protruding particles were related with particle adhesion, dispersed arrangement and filling up on planar substrate surface during repeated coating. So it resulted that the size and number of protruding particles were directly affected to the surface roughness of coated surface.

From the investigation of the relation with coating times and surface roughness on coated surface, 4 times coating specimen showed maximum surface roughness (Ra 0.36 μm in L powder, Ra 0.27 μm in T powder) in both types of 3Y-TZP powder as shown in Fig. 7. Also, surface roughness of coated layer from L powder was higher than that of T powder due to the rough surface by large protruding particles, regardless of coating times.

Conclusions

Zirconia slurry coatings were fabricated by spin coating using two sizes of commercial powder to enhance the surface roughness of 3Y-TZP substrate. Sintered coating layer with homogeneous microstructure, uniform thickness and high compactness could be obtained from spin coating of slurry, but physical properties of coated layer were dependent on the particle size in slurry and coating times. The coating thickness gradually increases with repeated coating times, but surface roughness of coated surface is dependent on the powder type and repeated coating times. Slurry coating containing large particles is more effective to improve the substrate roughness than that of small particles. We also confirmed that repeated slurry coating is available to increase the surface roughness of 3Y-TZP substrate, but limits the maximum roughness by the coating time due to the appearance condition of protruding particles on substrate surface. In this experiment, 4 times coating specimen showed maximum surface roughness (Ra 0.36 μm in L powder, Ra 0.27 μm in T powder) in both types of 3Y-TZP powder.

Acknowledgments

This work was supported by the National Research

Foundation of Korea (NRF) grant funded by the Korean government (MEST) (No. 2018-019041).

References

1. P. F. Manicone, I. P. Rossi, and L. Raffaelli, J. Dent. 35[11] (2007) 819-826.
2. R. B. Osman, and M. V. Swain, Mater. 8[3] (2015) 932-958.
3. J. Chevalier, and L. Gremillard, J. Am. Ceram. Soc. 92[9] (2009) 1901-1920.
4. M. Hisbergues, S. Vendeville, and P. Vendeville, J. Biomed. Mater. Res. Part B: Appl. Biomater. 88B[2] (2009) 519-529.
5. V. Lughi, and V. Sergo, Dent. Mater. 26[8] (2010) 807-820.
6. M. Stimmelmayr, S. Sagerer, K. Erdelt, and F. Beuer, Int. J. Oral. Maxillofac. Implants. 28[2] (2013) 488-493.
7. I. Denry, and J.R. Kelly, Dent. Mater. 24[3] (2008) 299-307.
8. S. Zinelis, A. Thomas, K. Syres, N. Silikasand, and G. Eliades, Dent. Mater. 26[4] (2010) 295-305.
9. L. Rimondini, L. Cerroni, A. Carrassi, and P. Torricelli, Int. J. Oral. Maxillofac. 17[6] (2002) 793-798.
10. I. Denry, Dent. Mater. 29[1] (2013) 85–96.
11. L. D. Liu, Y.H. Cheng, and W.C.J. Weic, J. Ceram. Process. Res. 20[4] (2019) 347-356.
12. A. Scarano, F.D. Carlo, M. Quaranta, and A. Piattelli, J. Oral. Implantol. 29[1] (2003) 8-12.
13. L. Sennerby, A. Dasmah, B. Larsson, and M. Iverhed, Clin. Implant. Dent. Relat. Res. 7[1] (2005) 13-20.
14. Y. I. Kim, S. H. Sung, S. M. Lee, S. H. Lee, B. S. Lim, J. S. Byun, C. Y. Hyun, Y. Hwang, and J. W. Byeon. J. Ceram. Process. Res. 13[1] (2012) s31-s36.
15. A. Afzal, Mater. Express. 4[1] (2014) 1-12.
16. J. Chevalier, Biomater. 27[4] (2006) 535-543.
17. H. J. Wenz, J. Bartsch, S. Wolfart, and M. Kern, Int. J. Prosthodont. 21[1] (2008) 27-36.
18. M. Gahlert, T. Gudehus, S. Eichhorn, E. Steinhauser, H. Kniha, and W.Erhardt, Clin. Oral. Implants. Res. 18[5] (2007) 662-668.
19. G. Soon, B. Pingguan-Murphy, K.W. Lai, and S.A. Akbar, Ceram. Int. 42[11] (2016) 12543-12555.
20. S. Roedel, J. C. M. Souza, F. S. Silva, J. Mesquita-Guimarães, M. C. Fredel, and B. Henriques, Ceram. Int. 44[11] (2018) 12496-12503.
21. D. Yamashita, M. Machigashira, M. Miyamoto, H. Takeuchi, K. Noguchi, Y. Izumi, and S. Ban, Dent. Mater. J. 28[4] (2009) 461-470.
22. R. Mai, C. Kunert-Keil, A. Grafe, T. Gedrange, G. Lauer, M. Dominiak, and T. Gredes, Ann. Anat. 196[6] (2012) 561-566.
23. H. W. Kim. H. E. Kim, and J. C. Knowles, J. Biomed. Mater. Res. B: Appl. Biomater. 70[2] (2004) 270-277.
24. C. Agrafiotis, A. Tsetsekou, and I. Leon, J. Am. Ceram. Soc. 83[5] (2000) 1033-1038.
25. J. C. Kim, D. Y. Lee, H. R. Kim, H. W. Lee, J. H. Lee, and J. W. Son, Thin. Solid. Films. 519[8] (2011) 2534-2539.
26. M. Norouzi, and A. A. Garekani, Ceram. Int. 40[2] (2014) 2857-2861.
27. D. S. Kim, and J. K. Lee, J. Nanosci. Nanotechnol. 19[2] (2019) 1118-1121.